# Hybrid Kalman Filter–Sliding Mode Observer for State-of-Charge Estimation in Lithium-Ion Batteries under Dynamic Load Conditions

RAGHAVENDAR INGUVA[1,2], K. SRINIVASA RAO[3], P. V. V. RAMA RAO[4,*]
[1]Department of EEE, GIETU,
Gunupur, Odisha,
INDIA

Department of Engineering & Technology,
University of Technology and Applied Sciences,
Nizwa,
OMAN

[3]Department of Electrical & Electronics Engineering,
Gunupur, Odisha,
INDIA

[4]Department of Electrical & Electronics Engineering,
MVSR Engineering College (A),
Hyderabad,
INDIA

[*]*Corresponding Author*

*Abstract:* - The estimation of State-of-Charge (SoC) is crucial for the safe and efficient operation of battery management systems (BMS), but no single method is able to reliably estimate the SoC under all operating conditions. In this paper, a hybrid estimator based on the Extended Kalman Filter (EKF) and Sliding Mode Observer (SMO) is presented by employing a gated bumpless-transfer switching technique for the SoC estimation of a Lithium-ion battery. The EKF generates accurate estimates when the operating condition is normal, and the SMO is triggered when the measurement innovation is larger than an adaptive threshold, enabling the EKF to provide accurate estimates when large initial SoC error, high measurement noise, and transient sensor faults exist. In this paper, a second-order RC equivalent circuit model (ECM) of a 2.6 Ah lithium-ion cell was used to implement the proposed hybrid estimator as well as the EKF-only, SMO-only, and Coulomb counting methods. The results indicate that the hybrid EKF–SMO estimator does not significantly outperform a well-tuned EKF in an ideal Gaussian noise environment; however, it is significantly more robust against faults in the sensors and large uncertainty, which is suitable for practical BMS applications.

*Key-Words:* - State of charge estimation, Battery management system, Extended Kalman filter, Sliding mode observer, Hybrid estimator, Lithium-ion battery, Dynamic load profile.

Received: May 8, 2026. Revised: July 9, 2026. Accepted: August 11, 2026. Published: November 6, 2026.

## 1 Introduction

The Battery Management System (BMS) is a crucial component in electric vehicles (EVs), grid energy storage (GES) solutions, and portable electronic devices to ensure safe and efficient operation of lithium-ion battery packs. State of Charge (SoC) estimation is one of the quintessential functions of a Battery Management System (BMS) and is vital for charge/discharge control, cell balancing, thermal control, and remaining range prediction. Because of this, SoC cannot be measured directly, but must be estimated in real-time from the measurement of the battery voltage, current, and temperature, by using a battery model and estimation algorithm.

Several methods for the estimation of SoC have been reported in the literature. The problem with Coulomb counting is that it gradually loses its accuracy over time because of its sensor bias,

integration error, and uncertainty in how much capacity a particular battery has [1]. The Extended Kalman Filter (EKF) [2], [3], [4] was introduced for battery management and, as described in [2], is a recursive estimation algorithm that integrates a model of the battery with voltage feedback to minimize drift. It is still one of the most popular model-based SoC estimation techniques [5], [6]. The EKF requires accurate process and measurement noise models, and it is assumed that the noise is Gaussian. These assumptions can be broken in practice due to sensor faults, problems with connections, temperature-dependent variations of parameters, and electromagnetic interference. The EKF is not the only method that can be modified to work without the Gaussian noise assumption; another alternative is the Sliding Mode Observer (SMO). They have good resistance to non-Gaussian disturbances and low computational complexity, but it has problems with chattering, and it generally does not have as good steady-state accuracy as a well-tuned EKF [7], [8], [9], [10]. The complementary strengths of the EKF and SMO motivate the development of hybrid EKF–SMO estimation approaches. Instead of relying on a single estimation method, a hybrid approach combines the high steady-state accuracy of the EKF under normal operating conditions with the robustness of the SMO when noise, uncertainties, or sensor faults reduce EKF performance. [11] proposed a hybrid SoC estimation method that combines an extended Kalman filter (EKF) and a sliding mode observer (SMO) using a switching function and a tracking closed-loop structure. The method was developed with a first-order equivalent-circuit model, where the inactive observer tracks the output of the active observer. This arrangement was used to benefit from the noise-filtering property of the EKF and the disturbance-rejection capability of the SMO. In the present study, a second-order RC equivalent-circuit model is used, and the observer mode is selected according to the measurement innovation. Specifically, the difference between the measured terminal voltage and the voltage predicted by the EKF is used as the basis for switching between the EKF and SMO. A hysteresis condition is included to prevent unnecessary switching when the innovation remains close to the switching threshold. The proposed estimator is evaluated under measurement noise, current drift, impulsive voltage disturbances, and sensor faults. Its sensitivity to SMO gain, boundary-layer width, initial SoC error, EKF process-noise covariance, and fault magnitude is also investigated. The resulting framework therefore considers innovation-based observer selection together with the effects of parameter variations and sensor disturbances on SoC estimation performance. Although previous studies have investigated fuzzy-tuned SMOs [7] and hybrid filtering approaches, limited work has systematically evaluated the conditions under which hybrid estimators provide measurable benefits, particularly under nominal operation, high uncertainty, and sensor faults.

The main contributions of this paper are as follows. First, a hybrid EKF–SMO estimator with a gated bumpless-transfer mechanism is developed. An adaptive innovation threshold, based on the voltage sensor noise level, selects the EKF or SMO at each sampling instant, while the inactive estimator is synchronized with the active one to ensure a smooth transition. Second, the proposed hybrid estimator is evaluated against EKF-only, SMO-only, and Coulomb-counting methods using a second-order RC equivalent circuit model of a 2.6 Ah lithium-ion cell. Performance is assessed under a one-hour dynamic drive-cycle current profile across two test conditions that distinguish nominal accuracy from robustness. Third, the study shows that the hybrid estimator matches the EKF under normal operating conditions while providing significantly improved robustness under sensor-fault conditions representative of practical BMS operation.

# 2 Battery Model and Estimator Formulation

## 2.1 Second-Order RC Equivalent Circuit Model

A second-order Thevenin's equivalent circuit model (ECM) was used to represent the electrical dynamics of the test cell, as it provides a good balance between modeling accuracy and real-time computational efficiency. Compared with first-order models, it captures transient behavior more accurately, while requiring significantly lower computational effort than electrochemical models, making it well suited for embedded BMS applications [12]. The state-space representation of the model is given by:

$$\mathrm{SoC(k+1)} = \mathrm{SoC(k)} - (\mathrm{I(k).\Delta t})/\mathrm{Q_n} \tag{1}$$

$$V_1(k+1) = a_1 * V_1(k) + R_1(1-a_1) * I(k), \quad a_1 = \exp(-\frac{\Delta t}{R_1 C_1}) \tag{2}$$

$$V_2(k+1) = a_2 * V_2(k) + R_2(1-a_2) * I(k), \quad a_2 = \exp(-\frac{\Delta t}{R_2 C_2}) \tag{3}$$

$$V_t(k) = OCV\big(SoC(k)\big) - I(k) * R_0 - V_1(k) - V_2(k) \tag{4}$$

where $V_1$ and $V_2$ are the polarization voltages of the short- and long-time-constant RC branches, respectively; $I(k)$ is the terminal current (positive during discharge); $Q_n$ is the rated battery capacity; $R_0$ is the ohmic resistance; and OCV (·) is the open-circuit voltage as a function of SoC, represented by a sixth-order polynomial fitted to a typical NMC/NCA lithium-ion cell. The model parameters used in this work are listed in Table 1.

Table 1. Battery Equivalent Circuit Model Parameters and Test Conditions

| Parameter | Value |
|---|---|
| Rated battery capacity, $Q_n$ | 2.6 Ah |
| Ohmic resistance, $R_0$ | 0.042 Ω |
| Short time-constant RC branch, $R_1/C_1$ | 0.018 Ω / 1800 F |
| Long time-constant RC branch, $R_2/C_2$ | 0.012 Ω / 9000 F |
| Current-sensor noise (nominal) | σ = 30 mA |
| Voltage-sensor noise (nominal) | σ = 4 mV |
| Test duration | 3600 s (1 h dynamic drive cycle) |

*Source: created by the authors*

### 2.2 Extended Kalman Filter (EKF) Formulation

The EKF estimates the state vector $[SoC, V_1, V_2]$ by linearizing the nonlinear $OCV(SoC)$ relationship at each sampling instant using its Jacobian, $\partial OCV/\partial SoC$. During the prediction step, the state and error covariance are propagated using the state-transition matrix A and process noise covariance Q. In the update step, the measurement innovation is computed from the difference between the measured and predicted terminal voltages, the Kalman gain is calculated, and the state estimate is corrected.

### 2.3 Sliding Mode Observer (SMO) Formulation

The SMO estimates the state using the same Coulomb-counting prediction as the EKF and corrects it using a bounded switching term based on the terminal voltage error, $e = V_{t,measured} - V_{t,predicted}$. To reduce chattering caused by the discontinuous sign function, a boundary-layer saturation function $sat(\frac{e}{\emptyset})$, is employed, where $\emptyset$ defines the boundary-layer width. Unlike the EKF, the SMO does not require a statistical noise model.

$$SoC\ (k+1) = SoC(k) - \frac{I(k)\cdot\Delta t}{Q_n} + k \cdot sat(\frac{e(k)}{\emptyset}) \cdot (\frac{\Delta t}{3600}) \tag{5}$$

### 2.4 Hybrid EKF–SMO Architecture (Gated Bumpless Transfer)

The proposed hybrid estimator executes the EKF and SMO simultaneously at each sampling instant. The EKF innovation magnitude, |y|, is compared with an adaptive threshold, $\gamma\sigma v$, where $\sigma v$ is the voltage sensor noise standard deviation and $\gamma$ is a tunable gain (set to 4 in this study). If |y| exceeds the threshold, indicating an outlier, large initial estimation error, or transient disturbance, the EKF update is skipped, and the estimator switches to the SMO.

## 3 Experimental / Simulation Setup

As a physical battery test bench was not available, the proposed method was validated using a high-fidelity simulation of the second-order RC equivalent circuit model described in Section II-A. The model was driven by a synthetic one-hour dynamic load current profile (3600 s, 1 Hz sampling) representing an urban driving cycle with cruising, acceleration, and regenerative braking.

A synthetic dynamic load current profile was generated using randomly selected current samples over a 60-min interval, with one sample assigned at each 1-min time step. The discrete samples were converted into a continuous-time current profile using standard piecewise-linear interpolation [13]. For $t_k \le t < t_{k+1}$, the interpolated current is defined as

$$I(t) = I_k + \frac{I_{k+1} - I_k}{t_{k+1} - t_k}(t - t_k) \tag{6}$$

where $I_k$ denotes the current sample at time tk. This approach provides a simple representation of time-varying load behavior while preserving the current variations between consecutive samples, [13].

Figure 1 shows the Synthetic load current profile plot used for validation.

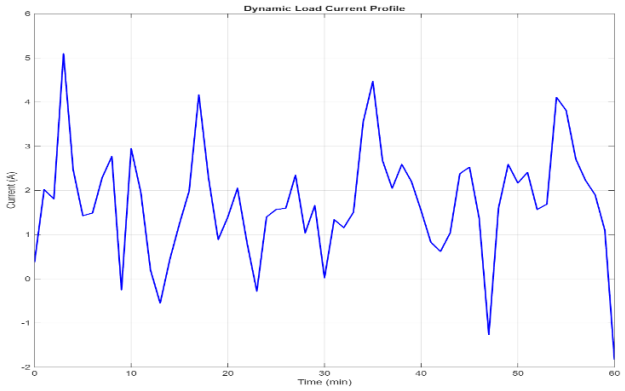



Fig. 1: Synthetic dynamic load current profile used for algorithm validation (I>0: discharge; I<0: regenerative charging).
*Source: created by the authors*

A net SoC change from 95% to approximately 27%. Simulation-based validation is widely used for evaluating SoC estimation algorithms before hardware-in-the-loop or experimental testing [5], [6], [10]. Accordingly, all results presented in this study were obtained directly from the implemented algorithms. The proposed approach provides an algorithm-level validation baseline. Before deployment in a practical BMS, it should be validated using an instrumented battery test bench to account for effects such as hysteresis, temperature-dependent parameters, and battery aging that are not included in the fixed-parameter ECM. The proposed method was evaluated under two test conditions: Nominal and Elevated Uncertainty.

To evaluate the performance of the proposed hybrid EKF-SMO estimator under transient sensor faults, two voltage disturbances were introduced in Condition B. The first disturbance was a positive bias of +300 mV, applied to the measured terminal voltage at 1800 s and maintained for 30 s, until 1830 s. The second disturbance was a negative bias of −250 mV, introduced at 2700 s and maintained for 20 s, until 2720 s. The disturbances were applied only to the measured terminal-voltage signal, while the true battery voltage remained unchanged. In addition to the transient faults, Condition B included increased current and voltage measurement noise, current-sensor drift, impulsive voltage disturbances, and a 10% initial SoC estimation error. The estimation performance of the EKF, SMO, and hybrid EKF-SMO estimators was evaluated during the fault intervals and after the faults were removed.

# 4 Results and Discussion

## 4.1 Condition A: Nominal Dynamic Load Tracking

Figure 2 shows that the four estimators do not converge to the reference SoC trajectory because of the uncorrected initial SoC offset and the current sensor drift under Condition A. The four estimators are unable to converge to the reference SoC trajectory due to the initial SoC offset (which is not corrected) and the current sensor drift.

In Figure 3, the estimation error is considered negative when the estimated SoC is below the reference SoC and positive when it is above the reference value. This sign convention is used consistently in the analysis of the SoC estimation results. The three closed-loop estimators (EKF, SMO, and Hybrid) are able to correct the initial estimation error and closely track the reference SoC trajectory. The EKF had the best performance; it had the fastest convergence and the lowest RMSE (0.11%) with the correct noise covariance matrices when operating under nominal conditions.

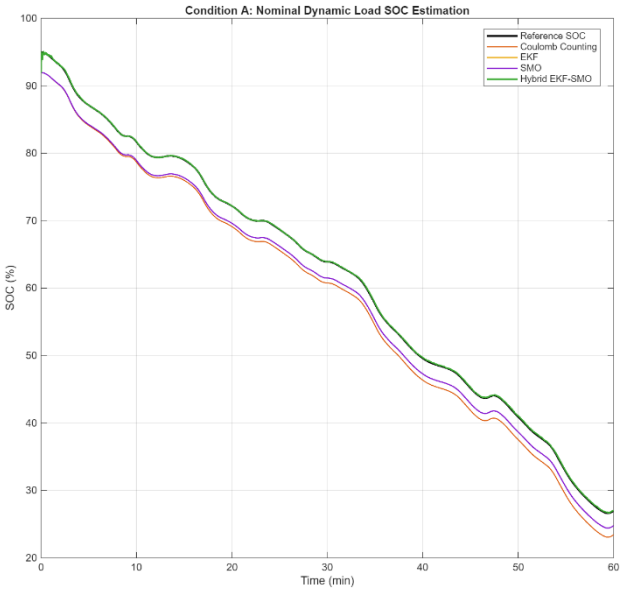



Fig. 2: SoC estimation performance under the nominal test condition (3% initial SoC estimation error)
*Source: created by the authors*

The SMO converged slower (87 s) and achieved a higher RMSE (2.49%), at the cost of robustness and steady-state accuracy. The hybrid estimator reduced the RMSE to 0.11% and the convergence time was 16 s, which is much faster than the convergence time of SMO (87 s) and is close to the EKF. The performance measures are summarized in Figure 4, and the switching behavior

of the hybrid estimator is shown in Figure 5. Most of the switching is in the convergence mode, and switching is rare in the steady-state mode. The EKF registered the smallest RMSE (0.103%) value when compared to the performance under Condition A. Table 2 shows the errors for different estimators.

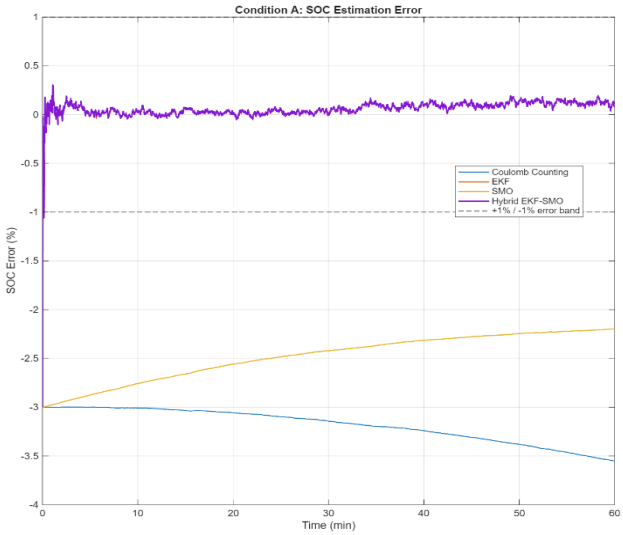



Fig. 3: SoC estimation error of the four estimators under Condition A. The dashed lines indicate the ±1% error band.
*Source: created by the authors*

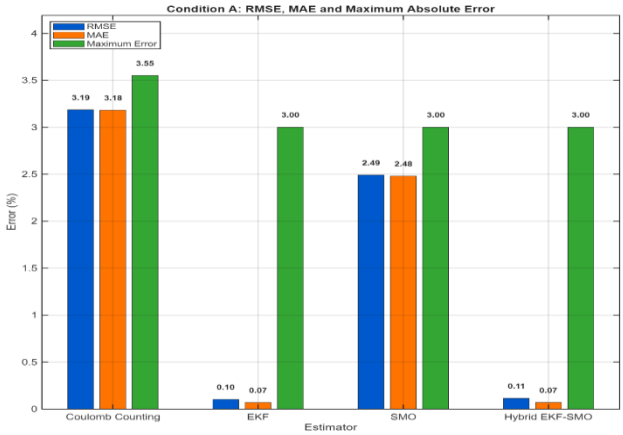



Fig. 4: Comparison of RMSE, MAE and maximum error for the four estimators under Condition A.
*Source: created by the authors*

Table 2. Comparison of errors for different estimators, Condition A

| Estimator | RMSE (%) | MAE (%) | Maximum Error (%) |
|---|---|---|---|
| Coulomb Counting | 3.19 | 3.18 | 3.55 |
| EKF | 0.103 | 0.07 | 3.0 |
| SMO | 2.49 | 2.48 | 3.0 |
| Hybrid EKF-SMO | 0.11 | 0.07 | 3.0 |

*Source: created by the authors*

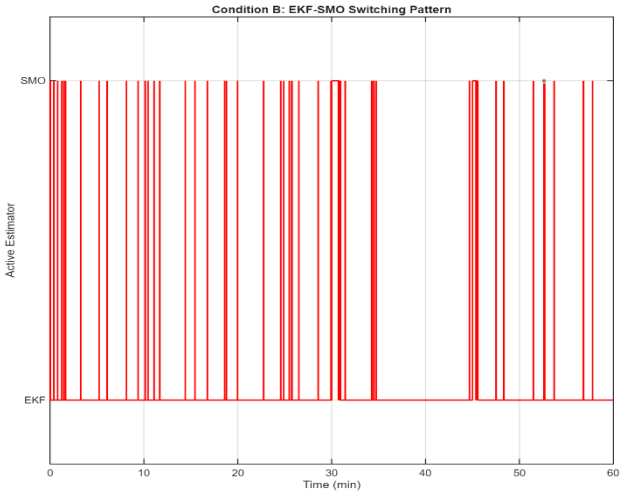



Fig. 5: Switching activity of the hybrid EKF–SMO estimator during the nominal drive cycle (1 = SMO update, 0 = EKF update).
*Source: created by the authors*

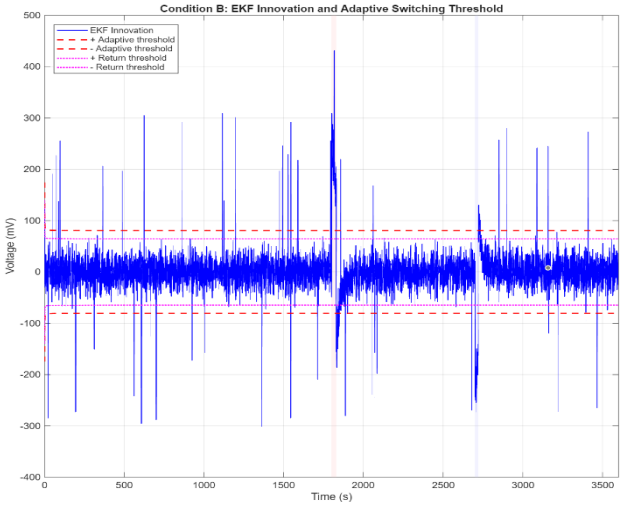



Fig. 6: Innovation-based switching behavior of the hybrid EKF–SMO estimator under elevated sensor noise and transient voltage faults.
*Source: created by the authors*

The Figure 6 emphasises the EKF innovation exhibits spikes exceeding the adaptive switching threshold during impulsive voltage disturbances and transient sensor faults, triggering a switch from EKF to SMO. The lower return threshold provides hysteresis, reducing frequent switching and improving robustness to non-Gaussian measurement disturbances.

## 4.2 Condition B: Elevated Sensor Noise and Larger Initial Error

The results indicate that the hybrid estimator is very accurate under a higher level of measurement noise when the process and measurement noise parameters are properly adjusted. The SMO had a higher RMSE (10.04%) and slightly slower

convergence when the measurement uncertainty was increased, which led to lower estimation accuracy when compared with the EKF. As shown in Figure 7, the hybrid estimator outperformed the SMO, reducing RMSE from 10.04% to 1.04% (89.64%) and MAE from 10.03% to 0.65% (93.52%). The hybrid estimator outperformed the EKF, reducing RMSE from 1.14% to 1.04% (8.77%) and MAE from 0.69% to 0.65% (5.8%). Table 3 shows the errors for different estimators.

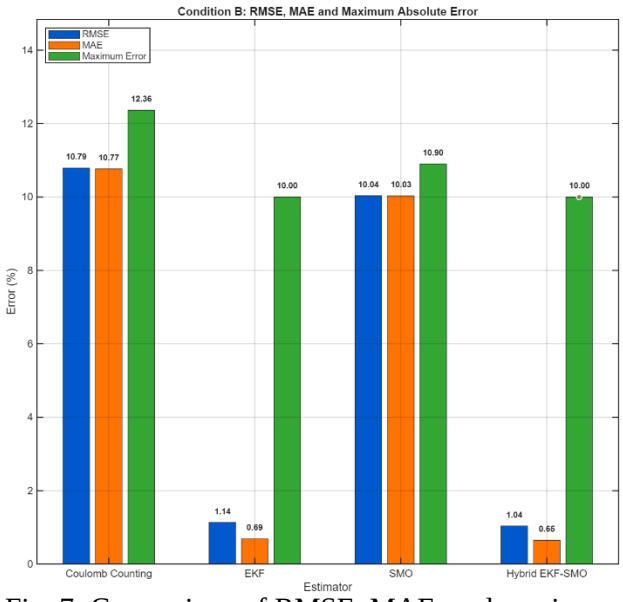



Fig. 7: Comparison of RMSE, MAE, and maximum error for the four estimators under Condition B.
*Source: created by the authors*

Table 3. Comparison of errors for different estimators under Condition B

| Estimator | RMSE (%) | MAE (%) | Maximum Error (%) |
|---|---|---|---|
| Coulomb Counting | 10.79 | 10.77 | 12.36 |
| EKF | 1.14 | 0.69 | 10 |
| SMO | 10.04 | 10.03 | 10.09 |
| Hybrid EKF-SMO | 1.04 | 0.65 | 10 |

*Source: created by the authors*

In general, the findings are clear and fair. The EKF under nominal operating conditions was the most accurate estimator, and the hybrid approach was not able to outperform it. The hybrid estimator was found to be most useful for abnormal operating conditions, like sensor disturbances and outliers in measurements.

It also outperformed the SMO in terms of accuracy in both test conditions. These results are more representative of the practical operation of BMS and are obtained in the presence of sensor disturbance, connector degradation, and electromagnetic interference, which illustrate the importance of the hybrid estimator in real-world scenarios. These results can then inform several possible future studies. The next step is to test the proposed estimator on a physical lithium-ion battery test bench to ensure that the simulation results agree with the actual values of the battery and the sensors. Additionally, further studies could be conducted on an automotive-grade embedded platform to compare the estimator against the EKF and SMO in terms of real-time performance and computational load.

In addition to the simulation done for different conditions, a sensitivity analysis is carried out to test the robustness of the hybrid EKF–SMO estimator for the following variations in different parameters and operating conditions. The variation range in RMSE is also indicated in Table 4.

Table 4. Comparison of errors for different estimators under Condition B

| Parameter | Range tested | RMSE variation range |
|---|---|---|
| SMO gain | 0.005–0.025 | 0.99% – 0.99% |
| Boundary-layer width | 0.005–0.025 | 0.97% – 0.97% |
| EKF Q scale | 0.25–4.00 | 0.78% – 1.67% |
| Initial SoC error | 2–10% | 0.94% – 0.96% |
| Sensor-fault magnitude | 100–500 mV | 0.52% – 1.65% |

*Source: created by the authors*

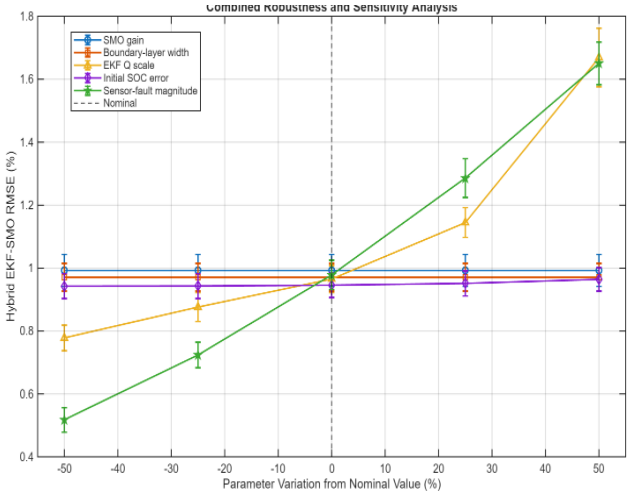



Fig. 8: Sensitivity analysis of SoC estimation performance under parameter variations and sensor-fault conditions.
*Source: created by the authors*

The Figure 8 presents the Sensitivity analysis of SoC estimation performance under different parameter variations and sensor-fault conditions. The sensitivity analysis indicated that the proposed hybrid EKF–SMO estimator is only marginally affected by changes in the SMO gain, boundary-layer width, and initial SoC error. In contrast, variations in the EKF process-noise covariance and sensor-fault magnitude have a more noticeable influence on the estimation accuracy. Despite this degradation under severe fault conditions, the SoC estimation error remains within an acceptable range throughout the tested cases, indicating that the proposed estimator can maintain reliable performance in the presence of parameter variations and sensor disturbances.

Future research can be performed to develop the proposed framework for simultaneous estimation of SoC, SoH, and internal resistance. A lightweight data-driven correction module can also be added to enhance the estimation accuracy under nominal operating conditions, whilst retaining the robustness when sensor disturbances occur.

# 5 Conclusion

This paper proposes and tests a hybrid EKF-SMO real-time state of charge (SoC) estimator for lithium-ion (Li-ion) batteries for gated bumpless transfer. The proposed estimator was tested under a second-order RC equivalent circuit model and a synthetic one-hour dynamic drive cycle, and compared to Coulomb counting, EKF, and SMO under two operating conditions with varying levels of uncertainty. The results demonstrate that the EKF has the best estimation accuracy for nominal operating conditions. During a transient sensor disturbance, however, the proposed hybrid estimator reduced the peak estimation error of the SoC and always performed better than the SMO under the test conditions considered. The results presented here prove the hybrid estimator EKF–SMO to be a practical compromise between accuracy and robustness. They also offer a good foundation for future experimental validation and adaptive tuning of the parameters.

**Declaration of Generative AI and AI-assisted Technologies in the Writing Process** During the preparation of this work, the author(s) utilized artificial intelligence (AI) technologies solely for the purpose of linguistic refinement and grammatical correction. Following the application of these tools, the author(s) comprehensively reviewed, verified, and edited the resulting text. The author(s) maintain full accountability and responsibility for the accuracy, integrity, and final content of the publication.

*References:*

[1] Movassagh, K., Raihan, S.A., & Balasingam, B. Krishna Pattipati (2021). A critical look at Coulomb counting towards improving the Kalman filter-based state of charge tracking algorithms in rechargeable batteries. arXiv:2101.05435. https://doi.org/10.48550/arXiv.2101.05435.

[2] Plett, G.L. (2004). Extended Kalman filtering for battery management systems of LiPB-based HEV battery packs: Part 1. Background. Journal of Power Sources, 134(2), 252–261. https://doi.org/10.1016/j.jpowsour.2004.02.031.

[3] Plett, G.L. (2004). Extended Kalman filtering for battery management systems of LiPB-based HEV battery packs: Part 2. Modeling and identification. Journal of Power Sources, 134(2),262–276. https://doi.org/10.1016/j.jpowsour.2004.02.032.

[4] Plett, G.L. (2004). Extended Kalman filtering for battery management systems of LiPB-based HEV battery packs: Part 3. State and parameter estimation. Journal of Power Sources, 134(2), 277–292. https://doi.org/10.1016/j.jpowsour.2004.02.033.

[5] Yuan, S., Wu, H., & Yin, C. (2013). State of charge estimation using the extended Kalman filter for battery management systems based on the ARX battery model. Energies, 6(1), 444–470. https://doi.org/10.3390/en6010444.

[6] Shrivastava, P., Soon, T.K., Idris, M.Y.I.B., & Mekhilef, S. (2019). Overview of model-based online state-of-charge estimation using Kalman filter family for lithium-ion batteries. Renewable and Sustainable Energy Reviews, 113. doi: 10.1016/j.rser.2019.06.040.

[7] Zheng W, Xia B, Wang W, Lai Y, Wang M, Wang H. State of Charge Estimation for Power Lithium-Ion Battery Using a Fuzzy Logic Sliding Mode Observer. Energies. 2019; 12(13):2491. https://doi.org/10.3390/en12132491.

[8] Behnamgol V, Asadi M, Mohamed MAA, Aphale SS, Faraji Niri M. Comprehensive Review of Lithium-Ion Battery State of Charge Estimation by Sliding Mode

Observers. Energies. 2024; 17(22):5754. https://doi.org/10.3390/en17225754.

[9] Dahmardeh, M. et al. (2025). Lithium-ion battery SoC estimation using adaptive sliding mode observer and wavelet transform. International Journal of Energy Research. https://doi.org/10.1155/er/5582881.

[10] Omid Rezaei, Hossein Azizi Moghaddam, Behnaz Papari, A fast sliding-mode-based estimation of state-of-charge for Lithium-ion batteries for electric vehicle applications, Journal of Energy Storage, Vol. 45, 2022, 103484, ISSN: 2352-152X, https://doi.org/10.1016/j.est.2021.103484.

[11] Awelewa A, Omiloli K, Samuel I, Olajube A and Popoola O (2023) Robust hybrid estimator for the state of charge of a lithium-ion battery. Front. Energy Res. 10:1069364. doi: 10.3389/fenrg.2022.1069364.

[12] Hu, X., Li, S., & Peng, H. (2012). A comparative study of equivalent circuit models for Li-ion batteries. Journal of Power Sources, 198, 359–367. https://doi.org/10.1016/j.jpowsour.2011.10.013.

[13] T. A. Driscoll and R. J. Braun, Fundamentals of Numerical Computation: Julia Edition. Philadelphia, PA, USA: SoCiety for Industrial and Applied Mathematics (SIAM), 2023, ISBN: 978-1-61197-700-4, doi: 10.1137/1.9781611977011.

**Contribution of Individual Authors to the Creation of a Scientific Article (Ghostwriting Policy)**

Raghavendar Inguva carried out literature review, algorithm and simulation, Dr. K. Srinivasa Rao has worked problem formulation, Rama Rao P.V.V has worked on the dynamic load conditions and was responsible for the result analysis.

**Sources of Funding for Research Presented in a Scientific Article or Scientific Article Itself**

This research did not receive any specific grant from funding agencies in the public, commercial, or not-for-profit sectors.

**Conflict of Interest**

The author declares no conflict of interest.

**Creative Commons Attribution License 4.0 (Attribution 4.0 International, CC BY 4.0)**

This article is published under the terms of the Creative Commons Attribution License 4.0
https://creativecommons.org/licenses/by/4.0/deed.en_US